

Analytical characterization of O₃ samples prepared for investigation of tropospheric heterogeneous reactions

Mihyeon Kim and Jong-Ho Park[★]

Department of Science Education, Chemistry Major, Jeonbuk National University, Jeonju 54896, Korea

(Received October 4, 2022; Revised October 11, 2022; Accepted October 14, 2022)

Abstract: In this study, ozone (O₃) samples were prepared for investigating the heterogeneous reactions between O₃ and tropospheric aerosols and were characterized by spectroscopic methods. O₃ generated from an ozone generator was purified by selective adsorption on refrigerated silica gel, followed by transfer to a sample bulb. The amount of UV light ($\lambda = 256$ nm) absorbed by O₃ was measured as a function of time at two different temperatures (room temperature and 50 °C) and under different irradiation conditions. A correlation plot of 1/[O₃] versus time showed that O₃ decomposition follows the 2nd order reaction rate under a steady-state approximation. The initial concentration of O₃, observed rate constants (k_{obs}), and the half-life of O₃ in the sample stored at room temperature were determined to be $2.74 [\pm 0.14] \times 10^{16}$ molecules·cm⁻³, $4.47 [\pm 0.64] \times 10^{-23}$ molecules⁻¹·cm³·s⁻¹, and 9.5 [± 1.4] days, respectively. The evaluation of O₃ stability under various conditions indicated that special care should be taken to prevent the exposure of the O₃ samples to high-temperature environment and/or UV radiation. This study established a protocol for the preparation of highly purified O₃ samples and confirmed that the O₃ samples can be stored for a day after preparation for further experiments.

Key words: Ozone, Stability of O₃, Troposphere, Heterogeneous reaction

1. Introduction

Ozone (O₃) is one of the most powerful oxidants in the troposphere.¹ O₃ plays an important role in homogeneous reactions as well as in heterogeneous reactions by oxidizing the surfaces of various tropospheric aerosols.²⁻⁵ As an example, organic aerosols are chemically activated by O₃ to shorten the length of the carbon chain or to bind oxygen atoms to molecules. This results in modified functional properties

of aerosols⁵ and eventually affects the chemical properties and concentrations of various tropospheric species of interest. The heterogeneous reactivity of O₃ is lower than that of hydroxyl radicals (OH radicals). However, the higher concentration of O₃ (by a factor of 10³–10⁵) contributes to the oxidation reactions in the troposphere in a manner comparable to that of OH radicals.⁶⁻⁸ Subsequently, information about kinetics and mechanism of the heterogeneous reactions of O₃ is important to update atmospheric models and

[★] Corresponding author

Phone : +82-(0)63-270-2814 Fax : +82-(0)63-270-2810

E-mail : proton@jbnu.ac.kr

This is an open access article distributed under the terms of the Creative Commons Attribution Non-Commercial License (<http://creativecommons.org/licenses/by-nc/3.0>) which permits unrestricted non-commercial use, distribution, and reproduction in any medium, provided the original work is properly cited.

gain better understanding of the atmosphere, especially the troposphere.

The prerequisite for the experimental investigation of the heterogeneous reactions of O₃ is the use of high-purity O₃ samples. Because O₃ is produced by an ozone generator that initiates production by the discharge of oxygen (O₂), the resulting O₃ is mixed with a large amount of O₂, which then needs to be removed from the samples for O₃ purification. One of the ways to selectively increase the O₃ content of samples is to utilize the difference in the boiling points between O₃ and O₂ (-112 and -183 °C, respectively). Therefore, O₃ can be separated from O₂ by adsorption on silica gel at a low temperature (approximately -100 °C).⁹ Due to its high reactivity and, thus, relative instability, the concentration of O₃ in the samples immediately decreases upon preparation. This implies that long-term storage of O₃ samples may not be possible and the evaluation of the O₃ samples is necessary to meet the experimental requirements.

In this technical note, the procedure for preparing purified O₃ samples using the fractional distillation technique is described in detail. Absorption spectroscopy using ultraviolet (UV) light was applied for the accurate measurement of the O₃ concentration and to derive the correlation between the concentration by estimation and measurement. The stability of the sample was estimated by a kinetic study, which provides preliminary information to design an experiment for studying the heterogeneous reaction of O₃ on tropo-

spheric aerosols, such as primary organic aerosols (POA) and secondary organic aerosol (SOA).

2. Experimental

2.1. Preparation and purification of O₃ samples

A vacuum line system, as shown in *Fig. 1*, was used for the preparation and purification of the O₃ samples. The vacuum line system consisted of a mixing chamber (AF-0061-03, Chemglass, USA), a pumping system equipped with a cold trap and mechanical pump (DUO 5M, Pfeiffer Vacuum Technology, USA), and four connection ports. An O₃ sample bulb (3 L, Home-made) was connected to the vacuum line system through a connection port (*Fig. 1*). A pressure gauge (275 Mini-Convenctron, MKS, USA) was used to monitor the pressure of the vacuum line system and estimate the O₃ concentration in the sample bulb.

O₃ was generated from the sequential reactions occurring in an ozone generator (LAB-1, Ozone Tech, Daejeon, Korea) connected to the O₃ trap. The reaction was initiated by the electrical discharge of oxygen flow (O₂, 99.999 %, 0.03 MPa, 1.5 L/min) to produce atomic oxygen [Reaction (1)], which combines with molecular oxygen to generate O₃ [Reaction (2)]. A small amount of O₂ participated in the generation of O₃; hence, the output was a mixture of O₃ and O₂ gases.

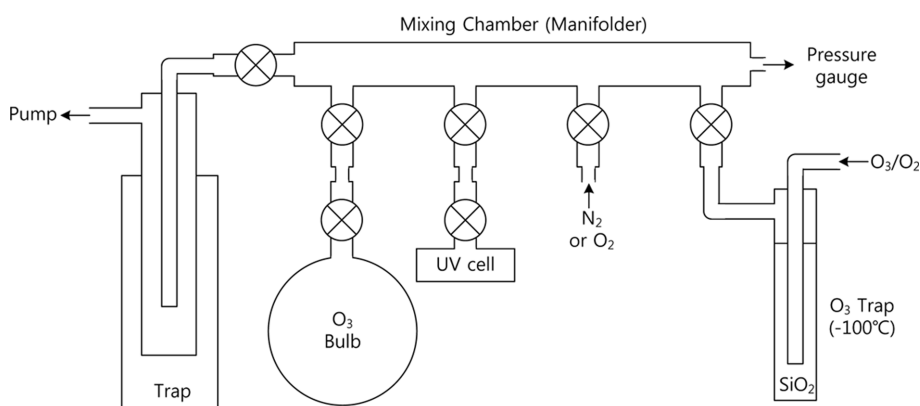
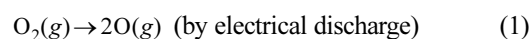
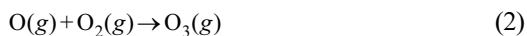


Fig. 1. Diagram of the vacuum line system.



An O₃ trap filled with silica gel (mesh size 15-25) was placed in a cold bath (8640, POPE Scientific Inc., USA), whose temperature was maintained at around -100 °C by using a mixture of ethyl alcohol (99.5 %, Samchun Inc, Korea) and liquid nitrogen. O₃ was introduced into the trap, followed by selective adsorption on the refrigerated silica gel surface, whereas most of the O₂ passed the O₃ trap without being adsorbed and was discarded. Upon the adsorption of O₃, the silica gel turned purple. After O₃ was collected for 10 min, the ozone generator was turned off and disconnected from the O₃ trap. The O₃ trap was then connected to the vacuum line system, which removed the other gaseous species (e.g., O₂) from the trap. The vacuum pump was closed once all the impurities were removed, and the cold bath was removed from the O₃ trap to desorb O₃ from silica gel by increasing the temperature. When the pressure of the vacuum line system reached ~1.5 Torr, the valve to the O₃ bulb was opened to fill O₃, followed by dilution with nitrogen (up to 700 Torr).

2.2. Characterization of O₃ samples

O₃ was transferred from the sample bulb to a homemade quartz UV cell (5 cm) by using a vacuum line system. The pressure drop in the sample bulb during the transfer was considered to estimate the partial pressure of O₃ in the UV cell. For the kinetic study, initial time ($t = 0$) was set as the moment O₃ transfer was completed. The initial concentration of O₃ in the UV cell ($[\text{O}_3]_0'$), which was equivalent to concentration of O₃ in sample bulb after the transfer, was calculated from the absorbance measured using a UV/Vis spectrophotometer (Cary 100, Agilent Technologies, USA). The cross section of O₃ by 256 nm light is 1.17×10^{-17} molecules⁻¹·cm².

The UV cell was then stored under the one of the following conditions:

- Condition 1 : Room temperature (~25 °C) with blocking external light using aluminum foil
- Condition 2 : High temperature (~50 °C) with blocking external light using aluminum foil
- Condition 3 : Room temperature (~25 °C) with UV light irradiation using a UV lamp (254 nm, < 0.1 mW, TN-4LC, Korea Ace Sci., Korea)
- Condition 4 : Room temperature (~25 °C) under a usual LED light condition (400 nm < λ < 800 nm)

The O₃ concentrations in the UV cell at various times were calculated using the method described above. The same method was used for kinetic studies of the O₃ samples stored under conditions 1-4 and in that order.

3. Results and Discussion

3.1. Initial concentration of O₃ in the sample

The initial concentration of O₃ (molecules·cm⁻³) in the sample ($[\text{O}_3]_0$) was determined by measuring the absorbance of O₃ in the UV cell. However, measuring the absorbance of each O₃ samples is not technically practical. On the other hand, estimating $[\text{O}_3]_0$ using the values of pressure measured during sample preparation is relatively feasible whereas the estimated values of $[\text{O}_3]_0$ may differ from the actual concentrations because of the existence of impurities, including O₂. The following equation was used for calculating $[\text{O}_3]_0$:

$$[\text{O}_3]_0 \text{ (molecules}\cdot\text{cm}^{-3}\text{)} = P_{\text{O}_3} \cdot c \cdot f \quad (3)$$

where P_{O_3} is the measured pressure (Torr) of O₃ in the sample bulb during preparation, c is the conversion factor (3.54×10^{16} molecules·cm⁻³·Torr⁻¹), and f is the correction factor. The correction factor, f , excludes the contribution of impurities as following:

$$f = \frac{P'_{\text{O}_3, \text{Abs}}}{P'_{\text{O}_3}} \quad (4)$$

P'_{O_3} and $P'_{\text{O}_3, \text{Abs}}$ are the partial pressures of O₃ in the UV cell measured by pressure and absorbance, respectively, as shown below:

$$P'_{\text{O}_3} = P_{\text{O}_3} \cdot \frac{P_{\text{Trans}}}{P_{\text{Prep}}} \quad (5)$$

$$P'_{\text{O}_3, \text{Abs}} = \frac{[\text{O}_3]_0'}{c} \quad (6)$$

where P_{Prep} and P_{Trans} are the total pressures (Torr) of the sample bulb measured during preparation and

transfer, respectively, and $[O_3]_0'$ is the initial concentration of O₃ in the UV cell, determined by absorbance.

The mean values of $[O_3]_0'$, P'_{O_3} , and $P'_{O_3, Abs}$ for four individual O₃ samples were $2.74 [\pm 0.14] \times 10^{16}$ molecules·cm⁻³, $1.60 [\pm 0.34]$ Torr, and $0.773 [\pm 0.004]$ Torr, respectively. Therefore, the correction factor was calculated to be $0.48 [\pm 0.11]$, which indicates that the O₃ concentration calculated from the pressure values was overestimated by a factor of $2.1 [\pm 0.5]$.

3.2. Half-life of O₃ in the samples

O₃ typically decomposes by the following mechanism:



where M is gaseous matter (N₂, O₂, or O₃, in this case); k_1 , k_2 , and k_3 are the rate constants for Reactions (7), (8), and (9), respectively. Reaction (9) was the rate-determining step.

The reaction rates involving O and O₃ are as follows:

$$\frac{d[O]}{dt} = k_1[O_3][M] - k_2[O_2][O][M] - k_3[O_3][O] \quad (10)$$

$$\frac{d[O_3]}{dt} = -k_1[O_3][M] + k_2[O_2][O][M] - k_3[O_3][O] \quad (11)$$

As atomic oxygen (O) is the intermediate of the mechanism (the steady-state approximation) and Reaction (9) is the rate-determining step (i.e., $k_3[O_3] \ll k_2[O_2][M]$), Eq. (11) can be rewritten as follows:

$$\frac{d[O_3]}{dt} = \frac{-2k_1k_3[M][O_3]^2}{k_2[O_2][M] + k_3[O_3]} = -k_{obs}[O_3]^2 \quad (12)$$

$$k_{obs} = \frac{2k_1k_3}{k_2[O_2]} \quad (13)$$

where k_{obs} is the observed rate constant of O₃ decomposition.

Eq. (12) shows that the decomposition of O₃ follows the 2nd order reaction rate, and the half-life ($t_{1/2}$) is equal to $1/(k_{obs}[O_3]_0')$. Fig. 2 shows the correlation

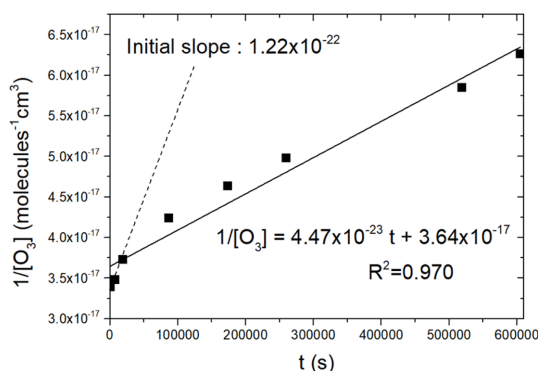


Fig. 2. Plot of $1/[O_3]$ versus time(s). The solid line and the dashed line represent the linear regression and the initial slope, respectively.

between $1/[O_3]$ and time (s) for the O₃ sample stored under Condition 1. The slope of the linear regression (the solid line in Fig. 2, which is 4.47×10^{-23} molecules⁻¹·cm³·s⁻¹) is equal to the value of k_{obs} . Moreover, the average value of $[O_3]_0'$ was calculated as 2.74×10^{16} molecules·cm⁻³, and the half-life of O₃ in the sample stored under Condition 1 was estimated to be $9.5 [\pm 1.4]$ days. Assuming that ~10 % change in the O₃ concentration is acceptable for heterogeneous reaction experiments, the O₃ sample can be stably used for one day after preparation.

3.3. Initial concentration of O₂ in the sample

Although linear regression showed a reasonably good fit ($R^2 = 0.970$), the plot for the early decomposition (i.e., $t < 10000$ s) deviated significantly from linearity, as shown in Fig. 2. The accumulation of O₂ by Reaction (9) is responsible for this deviation because k_{obs} is not a constant value. As k_{obs} is a function of the O₂ concentration [Eq. (13)], the initial concentration of O₂ in the UV cell ($[O_2]_0'$) can be estimated from the value of instantaneous k_{obs} at $t = 0$ (denoted as $k_{obs,0}$) using Eq. (12).

$$[O_2]_0' = \frac{2k_1 \cdot k_3}{k_2 \cdot k_{obs,0}} \quad (14)$$

The first two points in Fig. 2 denote the first two O₃ concentrations in the sample, representing the initial decomposition of O₃. Therefore the slope between the first two points (dashed line, 1.22×10^{-22} molecules⁻¹

$\cdot\text{cm}^3\cdot\text{s}^{-1}$) is assumed to be equal to $k_{obs,0}$. By applying the literature values for k_1 , k_2 , and k_3 (4.38×10^{-26} molecules $^{-1}\cdot\text{cm}^3\cdot\text{s}^{-1}$,¹⁰ 5.92×10^{-34} molecules $^{-2}\cdot\text{cm}^6\cdot\text{s}^{-1}$,¹¹ and 8.34×10^{-15} molecules $^{-1}\cdot\text{cm}^3\cdot\text{s}^{-1}$,¹² respectively) to Eq. (14), $[\text{O}_2]_0'$ was estimated to be 1.01×10^{16} molecules $\cdot\text{cm}^{-3}$, which is approximately 36.9% of $[\text{O}_3]_0'$. This implies that the overestimation of $[\text{O}_3]_0'$, when measured from the pressure values, was partially due to the existence of initial O_2 (O_2 at the moment the O_3 transfer was completed) in the sample. Considering that the major component in the output flow from the ozone generator was O_2 , the ratio of $[\text{O}_2]_0'/[\text{O}_3]_0'$ in the O_3 sample (and in the UV cell) showed that O_2 was efficiently removed from the O_3 sample by the purification process.

3.4. Stability of O_3 stored under various conditions

The k_{obs} and $t_{1/2}$ of the O_3 samples stored under four different conditions (Conditions 1-4) are summarized in Table 1.

The decomposition of O_3 was faster for the sample stored at 50 °C than that at room temperature, which resulted in a higher decomposition rate and reduction of the half-life to 4.0 days.

Unlike the sample stored under Condition 1, different irradiation environments were applied to the samples stored under Conditions 3 and 4. O_3 in the presence of UV light ($\lambda < 320$ nm) is decomposed by the following mechanism:¹

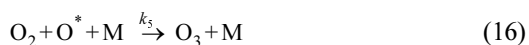


Table 1. k_{obs} and $t_{1/2}$ for the O_3 samples stored under various conditions

	k_{obs} (molecules $^{-1}\cdot\text{cm}^3\cdot\text{s}^{-1}$)	$t_{1/2}$ (day)
Condition 1	$4.47 [\pm 0.64] \times 10^{-23}$	$9.5 [\pm 1.4]$
Condition 2	$1.06 [\pm 0.04] \times 10^{-22}$	$4.0 [\pm 0.2]$
Condition 3	$4.22 [\pm 0.10] \times 10^{-20}$	$0.0100 [\pm 0.0006]$
Condition 4	$3.71 [\pm 0.66] \times 10^{-23}$	$11 [\pm 2]$

The numbers in parentheses indicate expanded uncertainty, $U = k \times u_c$, where u_c is the combined uncertainty and $k = 2$ with approximately 95% confidential level.



Therefore, Eq. (12) (the expression of O_3 decomposition rate) is rewritten as follow:

$$\frac{d[\text{O}_3]}{dt} = \frac{-2k_4k_6[\text{O}_3]^2}{k_5[\text{O}_2][\text{M}]} = -k'_{obs}[\text{O}_3]^2 \quad (16)$$

where, k'_{obs} is the observed rate constant of the O_3 decomposition in presence of UV light. This implies that the decomposition of O_3 in presence of UV light also follows the 2nd order reaction rate. Since k_4 and k_6 are much greater than k_1 and k_3 , respectively, and k_5 is smaller than k_2 (ie, $k_4 > k_1$, $k_6 > k_3$, and $k_5 < k_2$),^{11,13} k'_{obs} is considerably greater than k_{obs} as shown in Table 1. Consequently, half of the O_3 in the UV cell stored under Condition 3 decomposed within ~840 s. In contrast, no significant differences in the observed rate constant and half-life were observed under Conditions 1 and 4, based on the independent *t*-test with equal variance. This implies that LED light did not affect O_3 decomposition, and covering the samples with aluminum foil is not required even if the laboratory has an LED lighting system. However, blocking external light is still recommended to avoid any possibility of irradiation with indirect sunlight.

4. Conclusions

O_3 samples with high purity were prepared for studying the heterogeneous reactions of O_3 with tropospheric aerosols. To prepare purified O_3 samples, O_3 from an ozone generator was selectively adsorbed on refrigerated silica gel placed in a cold trap and then collected in an O_3 sample bulb.

The O_3 samples were characterized using a UV-Vis spectrophotometer to determine the actual $[\text{O}_3]$ in the samples and evaluate the stability of the samples. The consistent overestimation of $[\text{O}_3]$ calculated using the pressure values compared to that determined using the absorbance values was due to the presence of impurities, including O_2 , which were not removed during the purification process. This implies that a correction factor of 0.48 must be applied to $[\text{O}_3]$ calculated using the pressure values. The observed

rate constant of the O₃ decomposition and the half-life of O₃ in the samples were determined as 4.47 [± 0.64] $\times 10^{-23}$ molecules⁻¹·cm³·s⁻¹ and 9.5 [± 1.4] days at room temperature, respectively. The evaluation of O₃ stability under various conditions indicated that special care should be taken to prevent the exposure of O₃ samples to high-temperature environment and/or UV radiation.

Acknowledgements

This study was supported by “Basic Science Research Program” through the National Research Foundation of Korea (NRF) funded by the Ministry of Science and ICT (2019R1F1A1064144).

References

1. J. H. Seinfeld and S. N. Pandis, ‘Atmospheric Chemistry and Physics: from Air Pollution to Climate Change’, 4th Ed., Wiley, New York, 1997.
2. L. A. George, T. M. Hard and R. J. O’Brien, *J. Geophys. Res. Atmosphere*, **104**, 11643-11655 (1999).
3. B. J. Finlayson-Pits and J. J. N. Pits, ‘Chemistry of the upper and lower atmosphere’, 1st Ed., Academic Press, San Diego, 2000.
4. G. C. Morrison and C. J. Howard, *Int. J. Mass Spectrom. Ion Processes*, **201**, 503-509 (2001).
5. T. L. Eliason, J. B. Gilman and V. Vaida, *Atmos. Environ.*, **38**, 1367-1378 (2004).
6. A. K. Bertram, A. V. Ivanov, M. H. Hunter, L. T. Molina and M. J. Molina, *J. Phys. Chem. A*, **105**, 9415-9421 (2001).
7. J.-H. Park, A. V. Ivanov and M. J. Molina, *J. Phys. Chem. A*, **112**, 6968-6977 (2008).
8. J.-H. Park, C. I. Christov, A. V. Ivanov and M. J. Molina, *Geophys. Res. Lett.*, **36**, L02802 (2009).
9. G. A. Cook, A. D. Kiffer, C. V. Klumpp, A. H. Malik and L.A. Spence, *Ozone Chemistry and Technology*, **21**, 44-52 (1959).
10. J. M. Heimerl and T. P. Cofee, *Combust. Flame*, **35**, 117-123 (1979).
11. W. B. DeMore, S. P. Sander, D. M. Golden, R. F. Hampson, M. J. Kurylo, C. J. Howard, A. R. Ravishankara, C. E. Kolb and M. J. Molina, *JPL Publication 97-4*, 1-266 (1997).
12. R. Atkinson, D. L. Baulch, R. A. Cox, J. N. Crowley, R. F. Hampson, R. G. Hynes, M. E. Jenkin, M. J. Rossi and J. Troe, *Atmos. Chem. Phys.*, **4**, 1461-1738 (2004).
13. E. Castellano and H. J. Schumacher, *Z. Phys. Chem.*, **65**, 62-85 (1969).

Authors’ Positions

Mihyeon Kim : Graduate Student
Jong-Ho Park : Professor